FULL PAPER

ADVANCED FUNCTIONAL MATERIALS

DOI: 10.1002/adfm.200800165

Surface Engineered Carboxymethylchitosan/Poly(amidoamine) Dendrimer Nanoparticles for Intracellular Targeting**

By *Joaquim M. Oliveira, Noriko Kotobuki, Alexandra P. Marques, Rogério P. Pirraco, Johan Benesch, Motohiro Hirose, Silgia A. Costa, João F. Mano, Hajime Ohgushi,* and *Rui L. Reis**

Novel highly branched biodegradable macromolecular systems have been developed by grafting carboxymethylchitosan (CMCht) onto low generation poly(amidoamine) (PAMAM) dendrimers. Such structures organize into sphere-like nanoparticles that are proposed to be used as carriers to deliver bioactive molecules aimed at controlling the behavior of stem cells, namely their proliferation and differentiation. The nanoparticles did not exhibit significant cytotoxicity in the range of concentrations below 1 mg mL^{-1}, and fluorescent probe labeled nanoparticles were found to be internalized with highly efficiency by both human osteoblast-like cells and rat bone marrow stromal cells, under fluorescence-activated cell sorting and fluorescence microscopy analyses. Dexamethasone (Dex) has been incorporated into CMCht/PAMAM dendrimer nanoparticles and release rates were determined by high performance liquid chromatography. Moreover, the biochemical data demonstrates that the Dex-loaded CMCht/PAMAM dendrimer nanoparticles promote the osteogenic differentiation of rat bone marrow stromal cells, in vitro. The nanoparticles exhibit interesting physicochemical and biological properties and have great potential to be used in fundamental cell biology studies as well as in a variety of biomedical applications, including tissue engineering and regenerative medicine.

1. Introduction

Dendrimers are a relatively new class of synthetic,[1,2] highly branched, nanospherical, and low dispersity macromolecules.[3,4] They can be designed to provide quite a versatile choice of external functional groups in order to reduce cytotoxicity and enhance transepithelial transport,[5,6] and for interaction with coupling molecules such as natural-based polymers[7] and fluorescent probes,[8] and an inner hydrophobic core where other molecules can be trapped.[6] Among the myriad possibilities, dendrimers can find applications as delivery carriers of drugs[6,9] and DNA (transfection),[10] imaging agents,[11,12] and as tissue engineering scaffolding.[13] Although there are different routes to synthesize dendrimers,[4] their maximum size is typically in the order of ~10–20 nm.[12,14] Moreover, it has also been found[15] that high generation dendrimers (G7) with amine capping-groups cause haemolysis and changes in red cell morphology, and in general are overall cytotoxic. Therefore, the strategy proposed herein envisions the surface engineering of a dendrimer core grafted to natural-based and biocompatible polymers (linear polymer chains) in order to obtain copolymers of new architectures with tuned nanoparticle size and more versatile macromolecules. These should make it possible to avoid the cytotoxic effects of high-generation dendrimers. This new class of material is expected to exhibit entirely new properties since the structures might have sizes larger than 10 nm and different surface properties (dendronized polymer).[1] It is expected that the dendronized polymers developed in the present work will have potential applications as novel drug or gene delivery carriers for targeting certain tissues or cell cultures. Such nanodevices could display a higher loading capacity, and allow the bulk incorporation of bioactive molecules of higher molecular weights and of different chemistry, while maintaining high internalization and transfection efficiency as compared with conventional dendrimers.

In this study, novel water-soluble nanoparticles that consist of a poly(amidoamine) (PAMAM) dendrimer core with grafted carboxymethylchitosan (CMCht) chains (dendronized polymer) were successfully synthesized. They were then

[*] Prof. R. L. Reis, J. M. Oliveira, Dr. A. P. Marques, R. P. Pirraco
Dr. J. Benesch, Prof. S. A. Costa, Prof. J. F. Mano
3B's Research Group—Biomaterials, Biodegradables and Biomimetics
IBB—Institute for Biotechnology and Bioengineering
PT Government Associated Laboratory
Department of Polymer Engineering
University of Minho, Campus Gualtar, 4710-057 Braga (Portugal)
E-mail: rgreis@dep.uminho.pt
Dr. N. Kotobuki, Dr. M. Hirose, Dr. H. Ohgushi
Research Institute for Cell Engineering (RICE)
National Institute of Advanced Industrial Science and Technology (AIST)
Nakoji 3-11-46, Amagasaki, Hyogo 661-0974 (Japan)

[**] The authors acknowledge the financial support from the Portuguese Foundation for Science and Technology (FCT) and through POCTI and FEDER programs. The funding provided by Canon Foundation in Europe is gratefully acknowledged. This work was also carried out under the scope of the European *NoE* EXPERTISSUES (NMP3-CT-2004-500283) and HIPPOCRATES STREP project (NMP3-CT-2003-505758). Supporting Information is available online at Wiley InterScience or from the author.

ADVANCED FUNCTIONAL MATERIALS

characterized and screened for cytotoxicity using a fibroblast-cell line (L929) and rat bone marrow stromal cells (RBMSCs) by means of performing a tetrazolium reduction (MTT) assay and luminescent cell viability assay based on adenosine triphosphate (ATP) quantification, respectively. The internalization of fluorescein isothiocyanate (FITC)-labeled CMCht/PAMAM dendrimer nanoparticles was also investigated using both an osteoblastic cell line (SaOs-2) and RBMSCs as target cells. These types of cells are widely used in tissue engineering approaches[16,17] and are simple in-vitro systems for the assessment of the internalization efficiency of fluorescent-labeled molecules. It is our particular interest to engineer these nanoparticles to find applications in the intracellular controlled delivery of biological agents, including differentiation factors or genetic material, to modulate stem cell behavior while avoiding undesired secondary effects. In this context, the capacity of dexamethasone-loaded CMCht/PAMAM nanoparticles to promote the osteogenic differentiation of RBMSCs was also investigated. Alizarin red and alkaline phosphatase (ALP) stainings were carried out to qualitatively assess the mineralization capacity and ALP activity, which are known to denote the osteogenic differentiation. The quantitative content of ALP and osteocalcin, the early and late markers of osteogenic differentiation, respectively, were also determined.

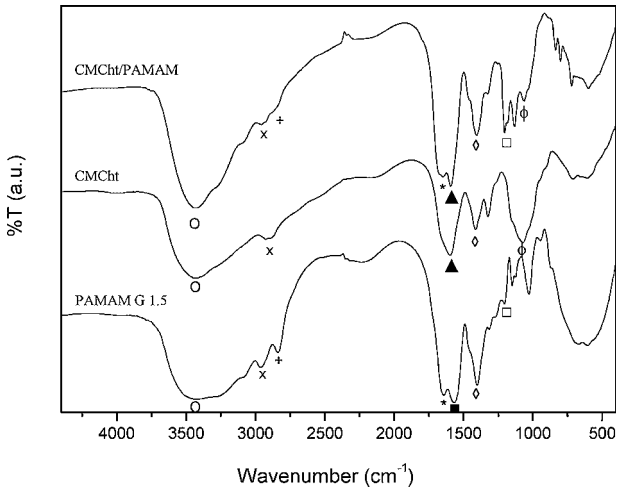

Figure 1. FTIR spectra of PAMAM G1.5, CMCht, and CMCht/PAMAM dendrimer nanoparticles. (O) 3450 cm^{-1} corresponds to –OH group, (x) 2996–2882 cm^{-1} is attributed to CH stretching bands, (+) 2860–2800 cm^{-1} corresponds to N–H stretching vibration, (*) 1655–1630 cm cm^{-1} corresponds to Amide I (ν C=O) (▲) 1570 cm cm^{-1} corresponds to Amide II (ν C–N and δ NH), (■) 1556 cm^{-1} is attributed to C–N stretching vibration (C–N bond inside the core), (◇) 1420 cm^{-1} corresponds to symmetric (s) stretching mode of COO^-, (□) 1200 cm^{-1} corresponds to C–N stretching vibration, and (ϕ) 1155 and 900 cm^{-1} corresponds to saccharine structure.

2. Results and Discussion

2.1. Characterization of the CMCht/PAMAM Dendrimer Nanoparticles

Figure 1 shows FTIR spectra of the PAMAM-CT dendrimers, CMCht, and CMCht/PAMAM dendrimer nanoparticles. The results suggest that CMCht was successfully synthesized, as evidenced by the presence of characteristic absorption bands of the carboxyl group at 1593 and 1420 cm^{-1} (ν_{as} COO^- and ν_s COO^-). The characterization of the molecular level conjugate obtained by the coupling reaction of CMCht with the PAMAM dendrimer was investigated by FTIR analysis. It was possible to detect characteristic absorption bands of groups attributable to both CMCht and the PAMAM dendrimer structure in the CMCht/PAMAM dendrimer nanoparticles. There is an increase in intensity of the bands at 1570 and 1200 cm^{-1} attributed to the amide II and C–N stretching vibrations, which is evidence that substituted amines are present and that there is possible chemical bonding between the CMCht and PAMAM. The effective degree of conjugation, measured by ^1H and ^{13}C NMR spectroscopy will be reported in a future work.

Some studies have shown that PAMAM is hydrolytically degradable because of its amide skeleton, and hydrolysis occurs slowly at physiological temperatures.[18] On the other hand, chitosan and its derivatives have been shown to possess bonds that are enzyme substrates.[19] Thus, the surface engineering of dendrimers proposed herein may furnish macromolecules with a different hydrolytic degradability, and may also release non-toxic products. As a consequence, the nanoparticles may show entirely new drug-delivery profiles and elimination rates. In preliminary degradation studies, a decrease was observed in the intensity of the band at 1655–1630 cm^{-1}, which corresponds to amide I (ν C=O) of the PAMAM dendrimer (see Supporting Information). Decreases are also detected in the band at 1200 cm^{-1} that corresponds to the C–N stretching vibration of the CMCht/PAMAM dendrimer nanoparticles, and those at 1155 and 900 cm^{-1}, attributed to the saccharine structure of CMCht. On the other hand, increased intensities of peaks attributed to the CH stretching bands and N–H stretching vibrations are observed. These preliminary data support the idea that the CMCht/PAMAM dendrimer nanoparticles are hydrolytically degradable at physiological temperature and pH, due to dissociation of their amide and glycosidic linkages. It has been shown that the architecture of nanoparticles strongly dictate the mechanisms and kinetics by which they are internalized by cells.[20–21] Gao et al.[20] have recently demonstrated that the optimal cellular uptake of particles by endocytosis occurs with particles that have diameters of ~50 nm. On the other hand, the mechanism of internalization of particles with larger diameters occurs preferentially by phagocytosis.[20] An atomic force microscopy (AFM) image of the CMCht/PAMAM nanoparticles is shown in Figure 2A. AFM characterization clearly demonstrates that the synthesized macromolecules consistently exhibit nanosphere-like shapes. It was also found that the CMCht/PAMAM dendrimer nanoparticles could be uniformly dispersed on a substrate by spreading a solution of dendronized polymers on a freshly cleaved mica surface and drying under a nitrogen gas stream.

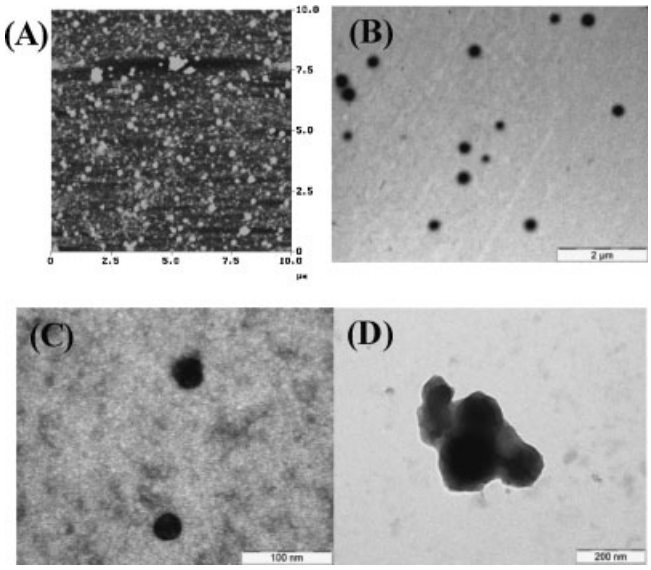

Figure 2. Representative A) AFM and B–D) TEM images showing the morphology of the CMCht/PAMAM dendrimer nanoparticles. A) The AFM images show a uniform nanoparticle distribution, where it is also possible to observe some aggregated nanoparticles. B) Low-magnification TEM image of the CMCht/PAMAM dendrimer nanoparticles. C) High-magnification TEM image of the CMCht/PAMAM dendrimer nanoparticles (~40 nm). D) TEM image of aggregated CMCht/PAMAM dendrimer nanoparticles (~250 nm).

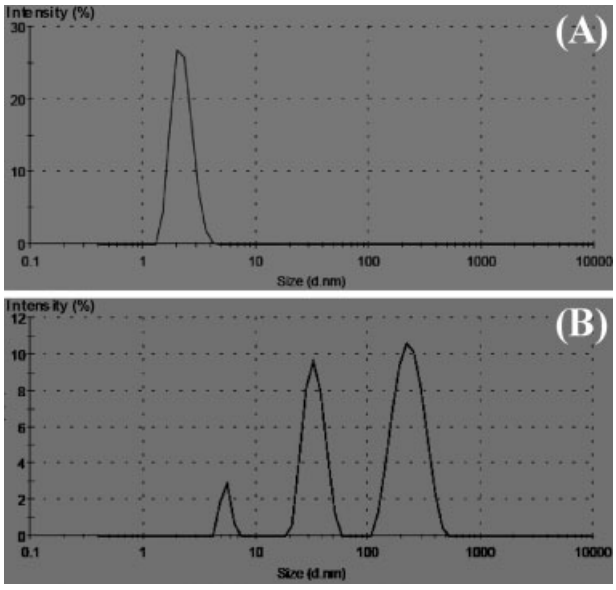

Figure 3. Particle size distribution of A) PAMAM G 1.5 and B) CMCht/PAMAM dendrimer nanoparticles.

The results of a morphometric analysis by AFM indicated that the nanoparticles have an average diameter of 26 nm (dry state) and average total area of ~2123 nm^2. These data were corroborated by transmission electron microscopy (TEM) observations. In Figure 2B,C it is possible to visualize the CMCht/PAMAM dendrimer nanoparticles in greater detail. It is also observed that the nanoparticles can form aggregates (Fig. 2D).

CMCht with a degree of deacetylation (DA) of 80% and a degree of substitution of 47% was used in the synthesis of the CMCht/PAMAM nanoparticles. Chitosan with a high degree of acetylation is insoluble in water because the acetylated units can be involved in intramolecular hydrogen linkages, which in part explains the insolubility of chitosan in water.[22]

Nevertheless, the modification of amino groups with carboxylic groups allowed us to obtain CMCht, a water-soluble chitosan derivate. Using potentiometric titrations it was possible to verify that the precipitation of CMCht occurred preferentially in a pH range from ~2–6 (data not shown). Thus, CMCht possesses protonated amino groups at pH 2, and negative COO^- ions at physiological pH. In other words, at physiological pH the CMCht behaves as a weak polyanionic polyelectrolyte, i.e., the amino groups are not protonated and most of carboxy groups are not dissociated. Interactions between non-covalent free carboxy groups of CMCht and/or the PAMAM-CT dendrimer and amino groups of other CMCht particles are possible, which may explain the formation of nanoparticle aggregates. It is worth noting that Zhu et al.[23] proposed the use of CMCht aggregates for the effective loading and controlled release of drugs. On the other hand, during the synthesis of CMCht/PAMAM dendrimer nanoparticles, there are several binding points available onto which possible cross-linking reactions may occur. This may also explain the formation of nanoparticle aggregates. Nanoparticle aggregation might be prevented or minimized by optimizing the concentrations of both CMCht and PAMAM.

Figure 3 shows the data obtained from the particle size distribution analysis of the different nanoparticles in solution. Figure 3A shows the low dispersivity of the PAMAM-CT (G 1.5) dendrimers used in the synthesis of the CMCht/PAMAM dendrimer nanoparticles. These nanoparticles have a diameter of 2 ± 1 nm, which is in agreement with previously reported data.[24] After the synthesis of the CMCht/PAMAM dendrimer nanoparticles, three kinds of particulate structures could be detected with sizes of approximately 6 ± 2, 45 ± 15, and 250 ± 100 nm (Fig. 3B). The first peak has an intensity of 5.5% and should correspond to the modified dendrimer. The second (36.2%) corresponds to the isolated CMCht/PAMAM dendrimer nanoparticles, and the third (58.2%) to the aggregated nanoparticles. Mammalian cells are sensitive to the osmolality of the ambient medium, and variations of this property may affect cell morphology and cell growth. It is known that most cell culture mediums are produced to have a osmolality in the range of 270–330 mOsm kg^{-1}, since these values are acceptable for most cells.[25] In this study, Eagle's minimum essential medium (MEM) supplemented with fetal bovine serum (FBS) and antibiotic-antimycotic (A/B, standard) with an osmolality of 310 ± 2 mOsm kg^{-1} was used. The effect of the CMCht/PAMAM dendrimer nanoparticles on the osmolality of the culture media was also investigated, since the

ADVANCED FUNCTIONAL MATERIALS

addition of medium concentrates may increase the osmolality of the media. The osmolality of the culture medium that contained nanoparticles at a concentration ranging from 0.01 to 1 mg mL^{-1} was assessed to be 315 ± 2 mOsm kg^{-1}. Varying the concentration of the CMCht/PAMAM dendrimer nanoparticles did not significantly change the osmolality of media, which indicates that the cells are not cultured under osmotic stress.

2.2. Cytotoxicity Screening

The cell viability in this work was preliminarily screened by performing an MTT test, which is a quite reliable method for assessing cytotoxicity.[26,27] A L929 fibroblast cell line was exposed to different concentrations of CMCht/PAMAM dendrimer nanoparticles over a period of 24 h (see Supporting Information). Two polymers, water-soluble CMCht (linear polymer) and PAMAM-CT G 1.5 (spherical polymer), were selected for a comparative study considering the fact that biocompatibility is thought to be influenced by various characteristics including the polymer molecular weight, concentration, structure (linear, branched, cross-linked), surface charge density, and flexibility.[26,28–30] Results indicate that dendronized polymers at concentrations of 0.01 and 0.1 mg mL^{-1} do not induce any toxicity for the investigated culturing times. However, at a concentration of 1 mg mL^{-1}, after 24 h the viability of the L929 cells decreased in the presence of the CMCht/PAMAM dendrimer nanoparticles, which suggests moderate cytotoxic effects. These results agree with previous studies where the concentration was reported to affect the biocompatibility of polymers to a certain extent.[26,30] Moreover, our findings are also consistent with previous results which indicated that high-molecular-weight structures may exhibit more serious cytotoxic effects.[26] However, such trends are meaningful only when the same type of polymer is compared.

Figure 4 shows the luminescent cell viability assay that was carried out after culturing the RBMSCs in the presence of different concentrations of CMCht/PAMAM dendrimer nanoparticles for 24 and 72 h. This assay is a homogeneous method based on the quantification of ATP and thus is a more feasible test for assessing the cytotoxicity of materials, since it signals the presence of metabolically active cells. The luminescence signal is proportional to the amount of ATP, which in turn is directly proportional to the number of cells in the culture medium. Statistically, it is possible to observe that increasing concentrations of CMCht/PAMAM dendrimer nanoparticles did not affect the viability (ATP content) of RBMSCs after 24 h ($P > 0.05$). When culturing the RBMSCs in MEM and in the presence of CMCht/PAMAM dendrimer nanoparticles, a statistical increase in viability was observed from 24 to 72 h ($P < 0.0001$). A statistical difference on the viability of RBMSCs was not seen when culturing RBMSCs in the presence of MEM and CMCht/PAMAM dendrimer nanoparticles in the range of concentrations between 0.01 and 0.1 mg mL^{-1} after 72 h ($P > 0.05$). However, the viability of RBMSCs decreased by

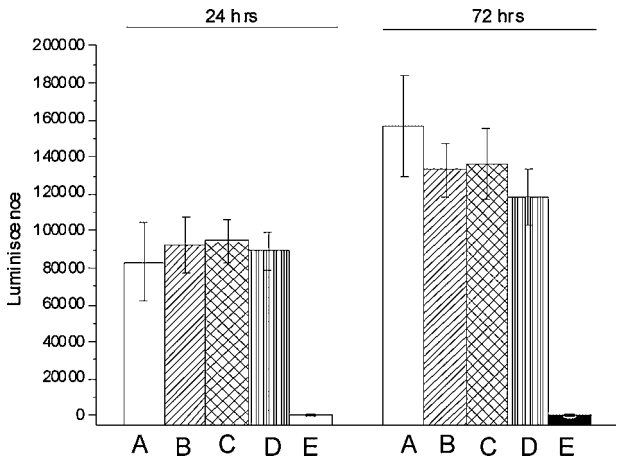

Figure 4. Viable RBMSCs after incubation in a culture medium with different concentrations of CMCht/PAMAM dendrimer nanoparticles for the period of 24 and 72 h. The cell number correlates with luminescence. A) MEM (negative control), B) 0.01, C) 0.1, and D) 1.0 mg mL^{-1} of CMCht/PAMAM dendrimer nanoparticles, and E) MEM that contained an latex extract (positive control) ($p < 0.0001$). Results expressed as an average $\pm$ standard deviation, $n = 12$. (Data were examined at a level of significance of $p < 0.05$.)

8.5% when culturing in the presence of 1 mg mL^{-1} of CMCht/PAMAM dendrimer nanoparticles ($P < 0.05$) as compared with the control. The latex extracts (positive control) have shown a high cytotoxic effect over RBMSCs, as seen by the low luminescence values after 24 and 72 h. These results demonstrate that RBMSCs remain viable in the presence of CMCht/PAMAM dendrimer nanoparticles at concentrations <1 mg mL^{-1}. Similar data were observed for the viability of L929 cells, which provides further evidence of the low cytotoxic effects of the CMCht/PAMAM dendrimer nanoparticles in the range of concentrations <1 mg mL^{-1}.

2.3. Internalization Efficiency of the CMCht/PAMAM Dendrimer Nanoparticles

Several studies [5,9,31,32] have been performed to clarify the entry and retention mechanisms of nanoparticles on mammalian cells as well as to investigate cell death.[33] For instance, it has been reported[5] that the cationic surface charge of particles is responsible for their interactions with the anionic glycoproteins and phospholipids of the cell membrane surface, which possibly facilitates their internalization. In the present case, it is expected that these types of interactions are responsible for the entry of CMCht/PAMAM dendrimer nanoparticles into the cell cytosol, either by passive transport caused through perturbations of the membrane or by endocytosis.[5] After being trapped within the endosome, the nanoparticles must be released into the cytosol before being subjected to acidic and/or enzymatic degradation. Nevertheless, because of the presence of protonated residues in the chain of the CMCht, which has a buffer capacity, it is expected that these nanoparticles can retard the degradation caused by acidification or enzymatic degradation within the endosomes. Theoretically, when loaded

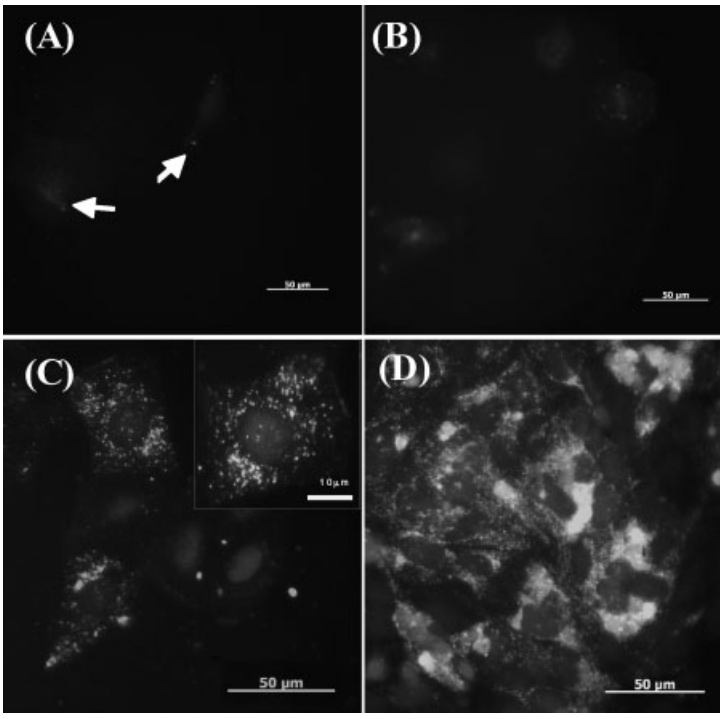

Figure 5. Fluorescence microscopy images of SaOs-2 cells after culturing in the presence of FITC-labeled CMCht/PAMAM dendrimer nanoparticles 1 mg mL^{-1} (green) for: A) 3 h, B) 12 h, C) 24 h, and D) 14 d. Nuclear DNA was labeled with DAPI (blue).

with drugs or DNA, this type of nanocarrier may increase the availability of drugs inside the cells or the transfection efficiency. In this study, the internalization and intracellular end-condition of the CMCht/PAMAM dendrimer nanoparticles were investigated by grafting a fluorescent label probe (FITC). This study was firstly performed using a SaOs-2 cell line and later on RBMSCs. Figure 5 shows the fluorescence microscopy images of SaOs-2 cells cultured in the presence of FITC-labeled CMCht/PAMAM dendrimer nanoparticles. The nanoparticles tested in this experiment consisted of the fraction of the total with size <220 nm, which was easily obtained by a filtration technique. It is apparent that CMCht/PAMAM dendrimer nanoparticles (green) are only present at the SaOs-2 cell membrane walls in low numbers after 3 h (white arrows), but in increasing amounts after a period of 12 h (Fig. 5A,B). However, after 24 h it is clearly seen that the CMCht/PAMAM dendrimer nanoparticles are internalized and widely distributed in the cytoplasm of the SaOs-2 cells (Fig. 5C). Moreover, there is also evidence of the presence of nanoparticles in the cell nuclei, as observed by the colocalization of the nuclei marker (blue) and FITC fluorescence (green). Cells continued to internalize the CMCht/PAMAM dendrimer nanoparticles (higher fluorescent signals) when cultured for longer periods of time, thus retaining their proliferation rate and remaining viable (Fig. 5D). A typical feature of apoptosis is the presence of chromatin condensation and nuclear fragmentation.[28] Apoptosis can be detected by nuclear morphology after staining with 4,6-diamidino-2-phenylindole dilactate (DAPI) blue or Hoechst 33258, for example. In Figure 5C,D, it is seen that SaOs-2 cells exhibit normal sized and round nuclei with homogeneous chromatin. Microscopic observations during the course of cell culturing in the presence of FITC-labeled CMCht/PAMAM dendrimer nanoparticles showed no morphological changes or cellular senescence, which is a good indication of cell survival. On the other hand, significant cell death was detected after 24 h for a culture of SaOs-2 cells in a media that contained FITC (control). These results also highlight the fact that the FITC-labeled CMCht/PAMAM dendrimer nanoparticles are quite stable, since their fluorescence was maintained over a period of 14 d. The fact that internalization of the nanoparticles was not well observed after 3 h can be attributed to the rather high detection limit of the fluorescence microscope. Fluorescent activated cell sorting (FACS) analysis was performed towards circumventing this limitation. In this analysis, primary cultures and FITC-labeled CMCht/PAMAM dendrimer nanoparticles at a concentration of 0.01 mg mL^{-1} were used. This concentration is impossible to detect by fluorescence microscopy and, therefore, makes a good test case for FACS.

Figure 6 shows the results of FACS analysis after culturing the RBMSCs in the presence of the FITC-labeled CMCht/PAMAM dendrimer nanoparticles for times up to 14 d. Flow-cytometry studies revealed increasing levels of fluorescence associated with cells after incubation of RBMSCs with CMCht/PAMAM dendrimer nanoparticles for the period of 12 h to 7 d. The present data show that nanoparticles were internalized with high efficiency by RBMSCs. The fraction of RBMSCs that internalized the nanoparticles reached 50.3% after 12 h and a maximum of 95.7% after 7 d of culturing (Table 1). At day 14, a decrease of

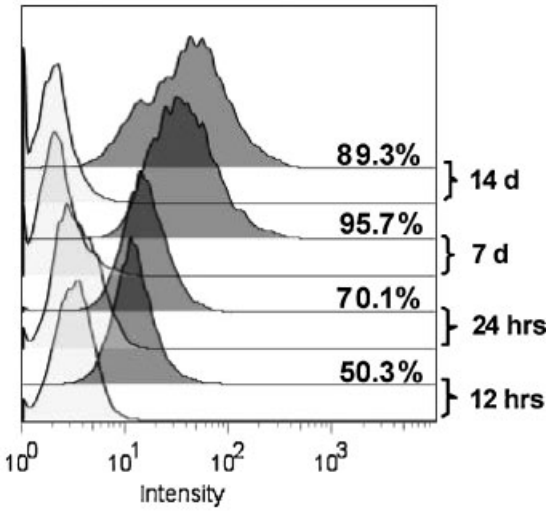

Figure 6. FACS data of live RBMSCs (% gated) after culturing in: MEM medium (light-grey peaks, control) and MEM medium with FITC-labeled dendrimer CMCht /PAMAM nanoparticles 0.01 mg mL^{-1} (dark-grey peaks) for the period of 12 h, 24 h, 7 d, and 14 d.

ADVANCED FUNCTIONAL MATERIALS

Table 1. FACS data of the percentage of internalization of FITC-labeled CMCht/PAMAM dendrimer nanoparticles by the fraction of live RBMSCs. The percentage of live cells (stained with PI) was obtained from the analysis of a total number of 10 000 cells per sample.

Culture conditions (medium)	Percentage of internalization (% gated)				Percentage of live RBMSCs (PI stained)			
	12 h	24 h	7 d	14 d	12 h	24 h	7 d	14 d
FITC-labeled CMCht/ PAMAM nanoparticles	50.3	70.1	95.7	89.3	96.0	93.7	75.4	62.6
MEM medium (control)	0.4	0.6	0.3	0.5	87.6	92.9	81.8	53.9

the internalization was detected, which may be related to the fact that RBMSCs reach confluence around day 7. Moreover, the RBMSCs were stained with propidium iodide (PI) to quantify the fraction of live cells.

From Table 1, it is concluded that the fraction of live cells cultured in the presence of FITC-labeled CMCht/PAMAM dendrimer nanoparticles did not significantly differ from that of the control. This result also demonstrates the biocompatible nature of the FITC-labeled CMCht/PAMAM dendrimer nanoparticles.

Fluorescence microscopy of RBMSCs cultured in the presence of FITC-labeled CMCht/PAMAM dendrimer nanoparticles corroborated the above-mentioned results of internalization studies carried out using a cell line, i.e., it confirmed that the nanoparticles were internalized and widely distributed in the cytoplasm of RBMSCs (Fig. 7). RBMSCs continued to internalize the nanoparticles (higher fluorescent signals) when cultured for longer periods of time. In addition, RBMSCs were also stained with Texas-red phalloidin for observation of the cell cytoskeletons. This makes it possible to assess whether the presence of the FITC-labeled CMCht/PAMAM dendrimer nanoparticles affects the cytoskeleton. It is known that cell mutations involve rearrangements and morphological modifications.[34] From careful examination it was concluded that no morphological changes could be detected compared with the control (data not shown). Interestingly, it appears that the FITC-labeled CMCht/PAMAM dendrimer nanoparticles are confined inside vesicular bodies that resemble endosomes. This observation would support the idea that their transport may occur through an endocytotic transcellular pathway. As was also observed for SaOS-2 cells, there is evidence of the presence of nanoparticles in the RBMSCs nucleus.

2.4. Mechanism of CMCht/PAMAM Dendrimer Nanoparticles Internalization

In order to gain further insight into the internalization mechanism, complementary experiments were carried out. The in-vitro experimental design consisted of culturing the RBMSCs in the presence of FITC-labeled CMCht/PAMAM nanoparticles and restrictive endocytotic drugs such as colchicine.[5] It is known that colchicine binds tightly to microtubules to cause microtubule depolymerization, and by this mechanism affects endocytosis.

On the other hand, it has been reported[35,36] that the translocation of macromolecules larger than 10 nm from the cytoplasm to the nucleus is by active transport through the nuclear pore complex (NPC), whereas small molecules and proteins smaller than 20–40 kDa cross the 10 nm diameter channels of the NPC by passive diffusion. Thus, we also exposed the RBMSCs to apyrase, a nuclear translocator inhibitor that causes ATP depletion, to study whether this treatment affects translocation of the FITC-labeled CMCht/PAMAM nanoparticles from the cytoplasm to the nucleus.

Figure 8 shows the percentage of RBMSC-associated fluorescence as a result of nanoparticle internalization after culturing the cells in the presence and/or absence of the restrictive drugs, for periods of 12 h, 24 h, 7 d, and 14 d. The results show that when culturing the RBMSCs in the presence of colchicine (green peak), apyrase (dark-blue peak), or exposed to both (red peak), a decrease in nanoparticle internalization is always observed. In fact, when colchicine is not

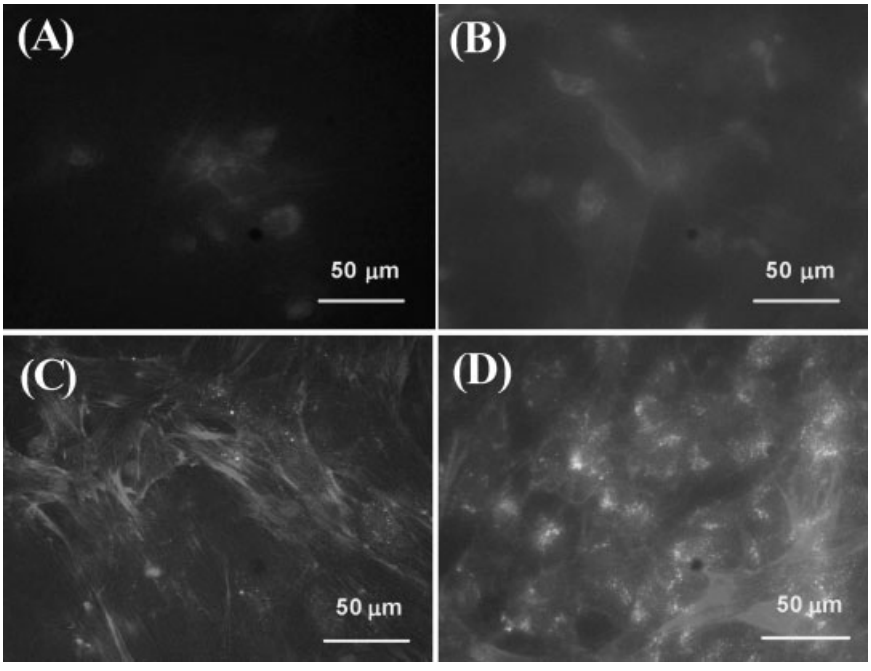

Figure 7. Fluorescence microscopy images of the RBMSCs cultured in the presence of FITC-labeled CMCht/PAMAM dendrimer nanoparticles 0.1 mg mL^{-1} (green) for: A) 12 h, B) 24 h, C) 7 d, and D) 14 d. Nuclear DNA and cytoskeleton were labeled with Hoechst 33258 (blue) and Texas-Red phalloidin (red), respectively.

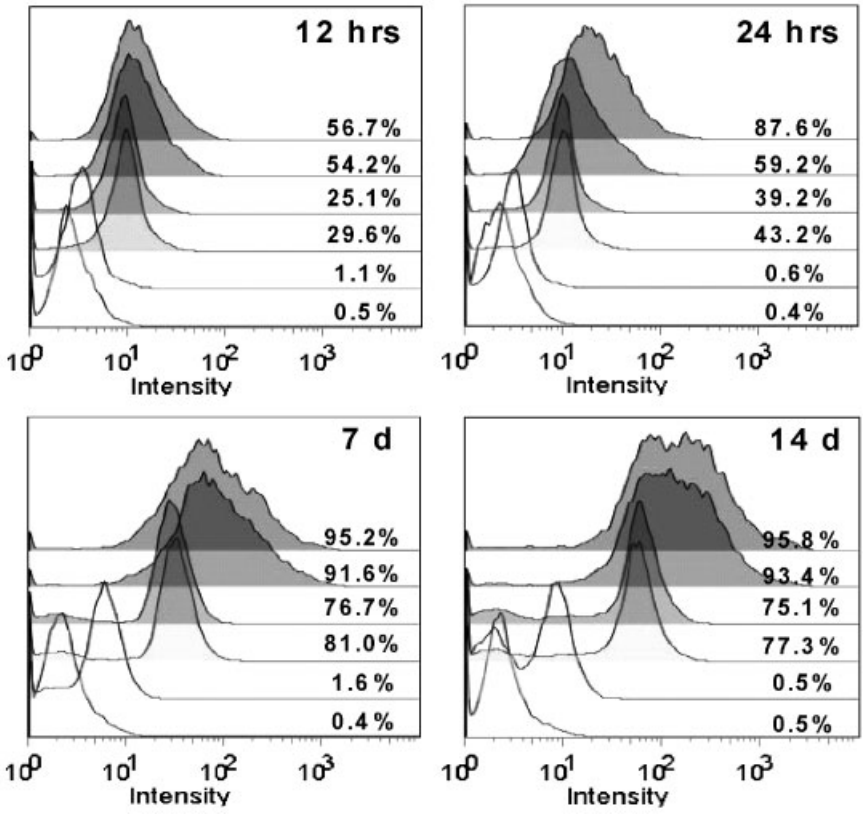

Figure 8. FACS data of RBMCS-associated fluorescence (% gated) after culturing in different culture media for 12 h, 24 h, 7 d, and 14 d. MEM (yellow). MEM with 0.1 U mL^{-1} apyrase and 1×10^{-6} M colchicine (light-blue). MEM that contained 0.01 mg mL^{-1} of FITC-labeled CMCht/PAMAM dendrimer nanoparticles and 1×10^{-6} M colchicine (green). MEM that contained 0.01 mg mL^{-1} of FITC-labeled CMCht/PAMAM dendrimer nanoparticles, 1×10^{-6} M colchicine, and 0.1 U mL^{-1} apyrase (red). MEM that contained 0.01 mg mL^{-1} of FITC-labeled CMCht /PAMAM dendrimer nanoparticles and 0.1 U mL^{-1} apyrase (dark-blue). MEM that contained 0.01 mg mL^{-1} FITC-labeled CMCht/PAMAM dendrimer nanoparticles (black).

present in the culture medium the nanoparticle internalization efficiency doubles for the culturing periods comprised of the first 24 h. However, the difference is not so pronounced after 7 and 14 d. Therefore, the present studies support the idea that not only nanoparticle internalization is highly dependent on the endocytosis mechanism, but also suggest that the nanoparticles enter the cells by a mechanism that might not be exclusively endocytotic. As previously discussed, the size of the nanoparticles strongly dictates the mechanism by which they are internalized.[20,37] The nanoparticles described herein have sizes that range from approximately 6 to 220 nm, and thus may be internalized by different mechanisms, i.e., cellular uptake of particles either by passive transport caused through perturbations of the membrane, endocytosis, and phagocytosis.[5,20]

On the other hand, FACS analysis showed that apyrase exposure did not affect nanoparticle internalization to a great extent after 7 and 14 d. However, after 24 h the observed internalization values with apyrase exposure (dark-blue peak) are significantly lower when compared with those of nanoparticle internalization without apyrase exposure (black peaks).

RBMSCs exposed to the restrictive drugs were also observed by fluorescence microscopy (Fig. 9). As shown in Figure 9C, it was observed that the FITC-labeled CMCht/PAMAM dendrimer nanoparticles were internalized and widely distributed in the cytoplasm of the RBMSCs, and the cells exhibited a normal morphology after 14 d. On the other hand, the depletion of ATP in the cells exposed to apyrase resulted in a decrease in nanoparticle internalization, which is more evident under fluorescence microscopy observation than by FACS analysis (Fig. 9D). A preferential localization around the perinuclear area was observed when the cells were treated with apyrase. It should be noted that the cells were not exposed to permeabilizing agents to avoid any undesired effects on the integrity of the cell nuclei. This result suggests that the presence of apyrase also prevents the nanocarriers from entering the cell nuclei, at least to a certain extent, since small molecules cross the 10 nm diameter channels of the NPC by passive diffusion. However, further complimentary studies are needed to clearly elucidate the possible localization of nanoparticles in the nucleus and whether nuclear import is an energy-dependent active process, since no ATP and/or GTP regenerating systems or temperature-dependent assays were carried out.[35,36] On the other hand, when colchicine was present in the culture medium a dramatic decrease in nanoparticle internalization was observed (Figs. 9E,F). In other words, the presence of colchicine restricted nanoparticle internalization. In addition, the exposure of RBMSCs to colchicine seems to prevent the formation of vesicular structures, as evidenced by the observation of uniform fluorescence of the FITC-labeled CMCht/PAMAM dendrimer nanoparticles around the perinuclear area. This assay further suggests that nanoparticles enter the cells by a mechanism that is not exclusively endocytotic. The colchicine treatment negatively affected cell growth, i.e., only a small number of stained nuclei were observed. The cytoskeleton morphology (Figs. B, E, and F) is also altered as evidenced by the increase in length of actin filaments when compared to that of the control (Fig. 9A). This is not surprising, since it is well known that colchicine disrupts the cytoskeleton.[38] Tsai et al.[39] reported that colchicine at concentrations less than 1×10^{-6} M caused disruption of microtubular structures of neutrophiles, but had little effect on either F-actin or on cellular mechanical properties. On the other hand, higher concentrations of colchicine disrupted the microtubular structure, but also caused increased actin

ADVANCED FUNCTIONAL MATERIALS

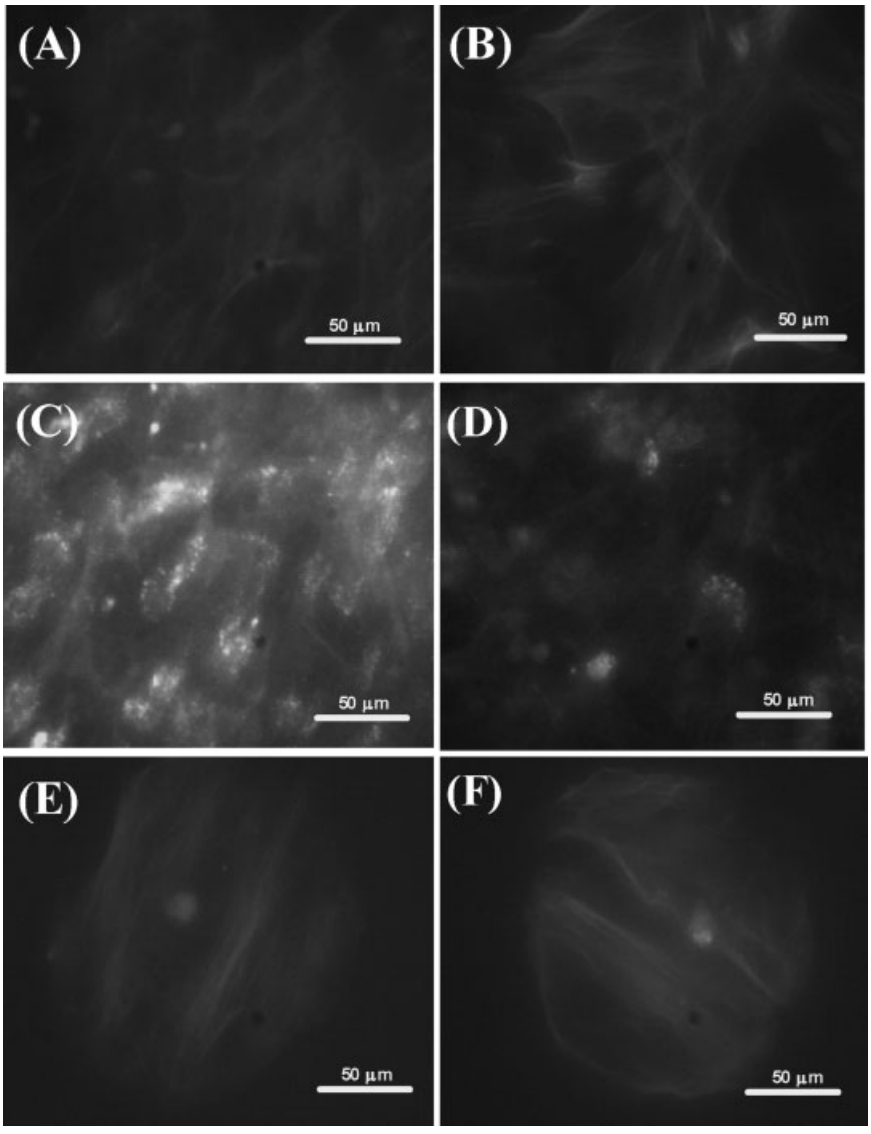

Figure 9. Fluorescence microscopy images of the RBMSCs cultured in different culture medium, after 14 d: A) MEM. B) MEM with 0.1 U mL^{-1} apyrase and 1×10^{-6} M colchicine. C) MEM with 0.1 mg mL^{-1} of FITC-labeled CMCht/PAMAM dendrimer nanoparticles. D) MEM with 0.1 U mL^{-1} apyrase and 0.1 mg mL^{-1} of FITC-labeled CMCht/PAMAM dendrimer nanoparticles. E) MEM medium with 1×10^{-6} M colchicine and 0.1 mg mL^{-1} of FITC-labeled CMCht/PAMAM dendrimer nanoparticles. F) MEM medium with 1×10^{-6} M colchicine, 0.1 U mL^{-1} apyrase, and 0.1 mg mL^{-1} of FITC-labeled CMCht/PAMAM dendrimer nanoparticles. FITC-labeled CMCht /PAMAM dendrimer nanoparticles (green). Nuclear DNA and cytoskeleton were labeled with Hoechst 33258 (blue) and Texas-Red phalloidin (red), respectively.

polymerization and cell rigidity. Thus, the present data demonstrate that the CMCht/PAMAM dendrimer nanoparticles have great potential for various applications as intracellular nanocarriers since they show properties useful for launching cell-impermeable drugs/DNA within target cells, for example. Moreover, in addition to their applications in intracellular drug-delivery systems, they can also be used for live-cell imaging during in-vitro culturing. It is further emphasized that the low toxicity of the CMCht/PAMAM nanoparticles is in contrast to those of most transfection agents and fluorescent labels, which exhibit significant cytotoxicity and have a period of use limited to only a few hours.[31,40]

By means of optimizing parameters such as the size and surface chemistry of the nanoparticles, we expect to develop more stable and versatile intracellular nanocarriers aimed at maximizing the drug availability to damaged tissues and decreasing the overall drug dosage and the need for frequent re-dosage, while simultaneously preventing drug exposure to healthy tissues.

2.5. In-Vitro Release of Dexamethasone from CMCht/PAMAM Dendrimer Nanoparticles

Glucocorticoids such as dexamethasone (Dex) have been shown[41–43] to promote the osteogenic differentiation of stem cells. On the other hand, glucocorticoids bind to the cytoplasmatic glucocorticoid receptor.[44,45] Therefore, Dex is an ideal drug to further investigate the loading and performance of the CMCht/PAMAM dendrimer nanoparticles as an intracellular drug-delivery system. Figure 10 depicts the Dex release profile from CMCht/PAMAM dendrimer nanoparticles at physiological pH. We have studied the effect of serum proteins on the retention of Dex by adding 15% FBS to a phosphate buffered saline (PBS) solution. An initial burst release of Dex is observed and the concentration reaches a maximum of 4 μg mL^{-1} in PBS with 15% FBS after 24 h. The release kinetics of Dex followed a steady release after the initial burst, which lasted for 7 d. This data shows that Dex is released as the free drug. The release of Dex from nanoparticles seems to be very slow for about 6 d after the initial release period, in the presence of serum proteins. By comparing the release rate of Dex in the absence of serum proteins, it can be seen that Dex is released more slowly after the initial burst period and a higher amount of Dex is still being released during this second stage. This data shows that the presence of serum proteins increases the initial amount of Dex released from the nanoparticles. This data is in agreement with a previous study,[46] and may be related to nanoparticle degradation by serum proteins. Despite this, further degradation studies need to be carried out to elucidate this issue. The timescale for the Dex release from the nanoparticles is of the same order of their internalization by

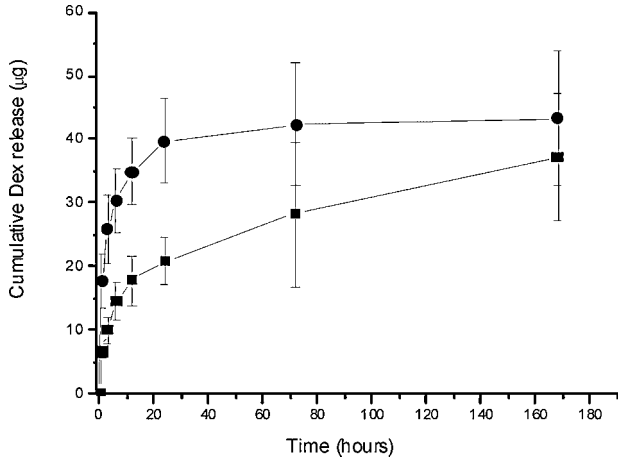

Figure 10. Dex release from 1 mg mL^{-1} of CMCht/PAMAM dendrimer nanoparticles at pH 7.4 (PBS buffer) in the presence (-●-) or absence (-■-) of 15% FBS under agitation at 37 °C, at 60 rpm, and determined by high performance liquid chromatography for periods between 1 h and 7 d. The results are expressed as an average ± standard deviation, $n = 6$.

cells. This could provide an indication of the retention of Dex within the nanoparticles in culture media and its release rate after it has been internalized by cells, in vitro. This and other issues, such as what will be the Dex release profile inside the endosomes (pH 5) and in in-vivo situations, remains to be examined in future studies.

2.6. In-Vitro Osteogenic Differentiation of RBMSCs Exposed to the CMCht/PAMAM Dendrimer Nanoparticles

An osteodifferentiation study is an interesting in-vitro model to validate the incorporation and release of Dex from the nanocarriers, since osteogenic differentiation varies with the dose and duration of exposure to the glucocorticoids.[41] On the other hand, in-vitro osteogenic differentiation of stem cells mimics many characteristics of the normal osteogenesis that occur in vivo. Under appropriate culture conditions, stem cells are induced to express osteogenic markers such as bone-specific ALP, osteopontin, and osteocalcin.[42,47] The deposition of an extracellular matrix, namely type I collagen, may occur, and as a consequence mineralization can be observed.[43,48,49] The presence of calcium is a late marker of osteoblast differentiation. In this work, the mineralization was qualitatively investigated using Alizarin red staining (Fig. 11). These results have shown that RBMSC cultures exposed to Dex-loaded CMCht/PAMAM dendrimer nanoparticles show high mineralization, as seen by the calcium staining (Figs. 11C,D). The extent of calcium deposition in cultures exposed to Dex-loaded CMCht/PAMAM dendrimer nanoparticles at a final concentration of 0.01 mg mL^{-1} was of the same magnitude as in cultures treated with standard culture media with Dex (osteogenic media), while RBMSCs cultured in the presence of CMCht/PAMAM dendrimer nanoparticles showed no mineralized nodules (Fig. 11B). This is an important result since it shows that incorporation of Dex and the nanoparticle concentration may influence the intensity and extent of mineralization. Moreover, an overall increase of calcium deposition in cultures exposed to Dex can be seen compared with those lacking the glucocorticoid (Figs. 11A, B, and F). The in-vitro release studies showed that the Dex concentration reaches a maximum of 4 μg mL^{-1} in PBS with 15% FBS after 24 h. Therefore, in a culture media with 0.01 mg mL^{-1} of Dex-loaded CMCht/PAMAM dendrimer nanoparticles, the concentration of Dex is expected to be in the magnitude of 40 ng mL^{-1} (10×10^{-9} M). Therefore, the Dex released from the CMCht/PAMAM dendrimer nanoparticles resembles that from osteogenic media. This range of concentrations of Dex has been shown to be effective for the osteogenic differentiation of MSCs.[41,50]

It is known that ALP, a cell surface glycoprotein, is an early marker of osteogenic differentiation.[47,51] To confirm the osteogenic differentiation of RBMSCs exposed to Dex-loaded CMCht/PAMAM dendrimer nanoparticles, we carried out an ALP staining (Fig. 12). As seen for calcium staining, the

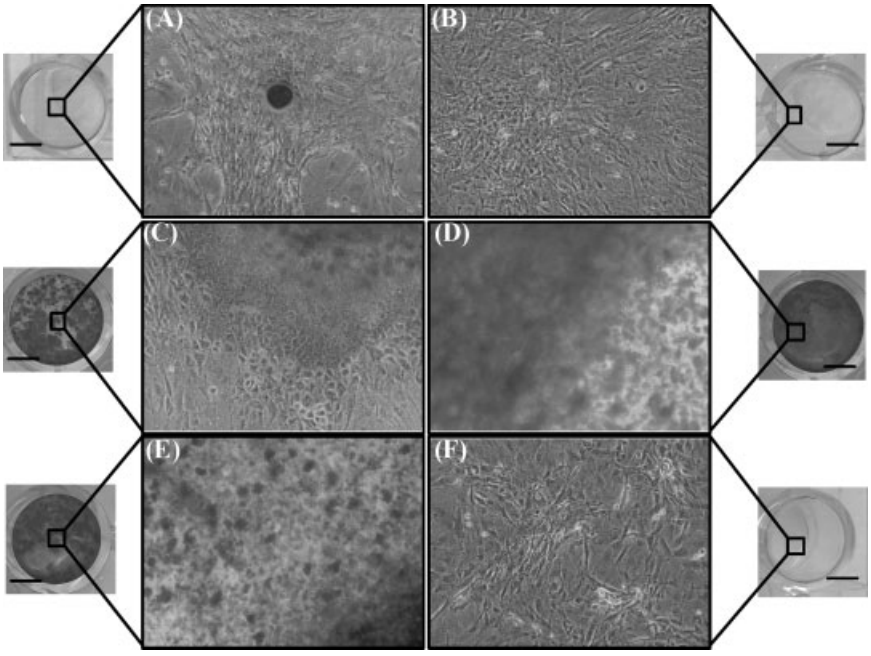

Figure 11. Calcium staining (Alizarin red) of RBMSCs after culturing in different culture medium for the period of 14 d. A) MEM (negative control). B) CMCht/PAMAM dendrimer nanoparticles (1 mg mL^{-1}). C) Dex-loaded CMCht/PAMAM dendrimer nanoparticles (1 mg mL^{-1}). D) Dex-loaded CMCht/PAMAM dendrimer nanoparticles (0.01 mg mL^{-1}). E) Osteogenic medium and F) MEM with β-glycerophosphate. (Original magnification: ×100, bar: 5 mm.)

ADVANCED FUNCTIONAL MATERIALS

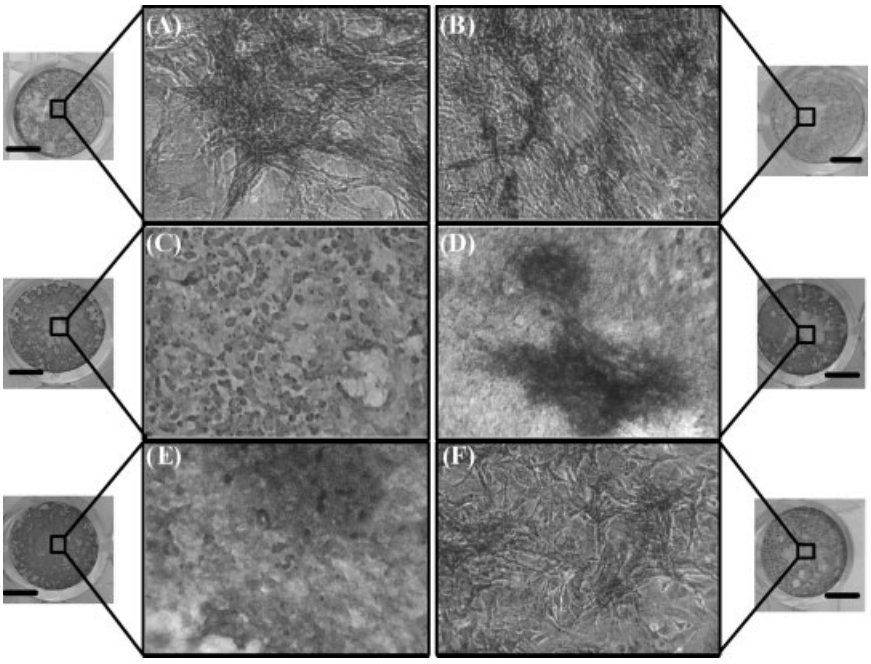

Figure 12. ALP staining of the RBMSCs cultured in different culture medium for the period of 14 d. A) MEM (negative control). B) CMCht/PAMAM dendrimer nanoparticles (1 mg mL^{-1}). C) Dex-loaded CMCht/PAMAM dendrimer nanoparticles (1 mg mL^{-1}). D) Dex-loaded CMCht/PAMAM dendrimer nanoparticles (0.01 mg mL^{-1}). E) Osteogenic medium and F) MEM with β-glycerophosphate. (Original magnification: $\times$100, bar: 5 mm.)

presence of cuboid-shaped clusters stained with ALP is higher in cultures exposed to Dex-loaded CMCht/PAMAM dendrimer nanoparticles (Figs. 12C,D). It is possible to observe a strong ALP staining in cultures with Dex-loaded CMCht/PAMAM nanoparticles at a concentration of 0.01 mg mL^{-1}. These results are further corroborated by the above mineralization data, which suggest that osteogenic differentiation of RBMSCs occurs in the presence of Dex-loaded CMCht/PAMAM dendrimer nanoparticles.

Figure 13 shows the quantitative analysis of ALP activity, both normalized for DNA content (left) and non-normalized (right). Cultures grown in the presence of standard medium, CMCht/PAMAM dendrimer nanoparticles, and β-glycerophosphate presented similar ALP activity. It can be seen that ALP activity is increased in cultures with Dex-loaded CMCht/PAMAM dendrimer nanoparticles. No statistical differences were observed for cultures grown in the presence of osteogenic medium and standard culture media with different concentrations of Dex-loaded CMCht/PAMAM dendrimer nanoparticles. As expected, we observed the up-regulation of ALP in the RBMSCs exposed to Dex. Dex consistently increased ALP activity, but it should be noted that Dex does not globally stimulate all genes considered to be part of osteoblast differentiation. On the other hand, the Dex actions are somehow species specific, or dependent on the culture conditions.[49]

The late osteogenic marker and bone-specific osteocalcin was also measured by performing an enzyme-linked immunosorbent assay (ELISA, Fig. 14). It is possible to observe that osteocalcin deposition occurs in cultures exposed to the Dex-loaded CMCht/PAMAM dendrimer nanoparticles.

In addition, higher osteocalcin content in cultures treated with osteogenic media can be seen. Despite this, the magnitude of osteocalcin deposition does not present significant differences when compared to that of cultures with 0.01 mg mL^{-1} Dex-loaded CMCht/PAMAM dendrimer nanoparticles. These observations can be explained by the fact that differentiation proceeds mineralization and the responsiveness of osteocalcin synthesis to long-term exposure to Dex, as this late marker appears to reach a maximum just before or during mineralized tissue formation.[52] Therefore, the present biochemical findings demonstrate that RBMSCs differentiate into osteoblasts and organize into a mineralized matrix when cultured in

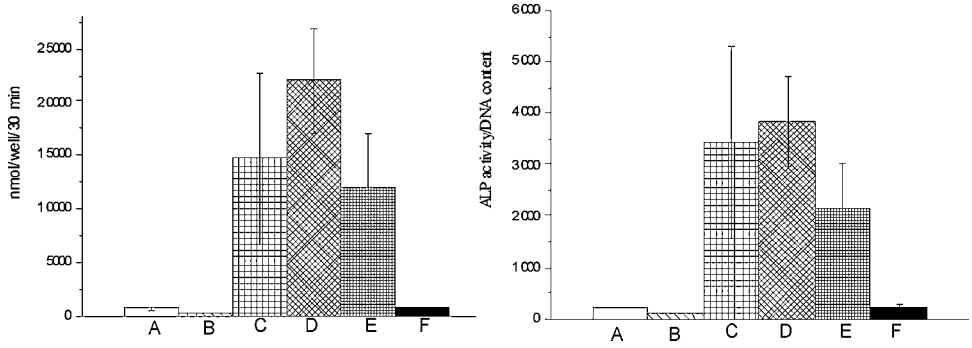

Figure 13. ALP activity (left) and ALP activity per DNA content (right) of RBMSCs cultured in the presence of different culture medium after 14 d. A) MEM (negative control). B) CMCht/PAMAM dendrimer nanoparticles (1 mg mL^{-1}). C) Dex-loaded CMCht/PAMAM dendrimer nanoparticles (1 mg mL^{-1}). D) Dex-loaded CMCht/PAMAM dendrimer nanoparticles (0.01 mg mL^{-1}). E) Osteogenic medium and F) MEM with β-glycerophosphate. Results expressed as an average $\pm$ standard deviation, $n = 12$.

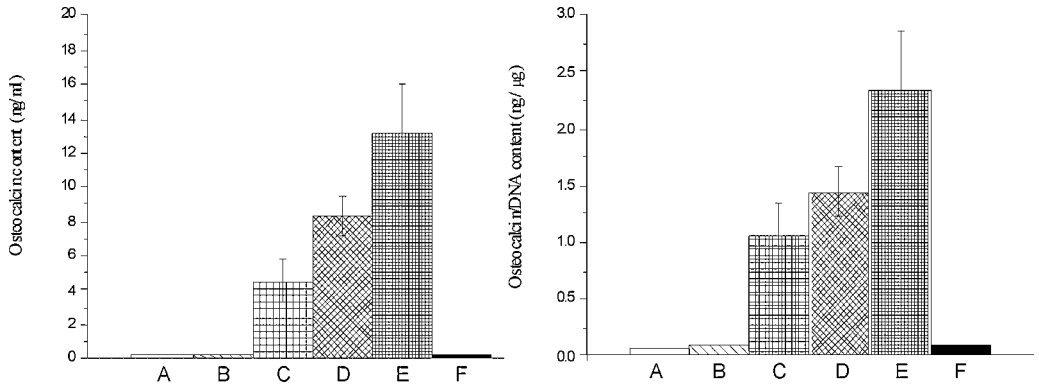

Figure 14. Osteocalcin quantification (left) and osteocalcin per DNA content (right) of RBMSCs cultured in the presence of different culture medium after 14 d. A) MEM (negative control). B) CMCht/PAMAM dendrimer nanoparticles (1 mg mL^{-1}). C) Dex-loaded CMCht/PAMAM dendrimer nanoparticles (1 mg mL^{-1}). D) Dex-loaded CMCht/PAMAM dendrimer nanoparticles (0.01 mg mL^{-1}). E) Osteogenic medium and F) MEM with β-glycerophosphate. Results expressed as an average $\pm$ standard deviation, $n = 12$.

the presence of Dex-loaded CMCht/PAMAM dendrimer nanoparticles.

While the intracellular Dex release profile is yet to be determined, the in-vitro release and differentiation studies have proved particularly useful to demonstrate that Dex was incorporated into the CMCht/PAMAM dendrimer nanoparticles and was released at a concentration that caused no negative effects on the RBMSCs osteogenic differentiation.

3. Conclusions

The results in this paper demonstrate that a combination of synthetic and natural-based polymers enables the preparation of CMCht/PAMAM dendrimer nanoparticles of suitable diameters to cover a wide range of intracellular delivery applications. In-vitro tests showed that the CMCht/PAMAM dendrimer nanoparticles do not exert any significant cytotoxic effect over both L929 fibroblast and RBMSCs for concentrations below 1 mg mL^{-1}.

Furthermore, the successful internalization of the nanoparticles by two different types of cells, i.e., cell lines and primary cultures, was also demonstrated. The biochemical data presented herein also proved that the Dex-loaded CMCht/PAMAM dendrimer nanoparticles induced the osteogenic differentiation of rat bone marrow stem cells in vitro. Therefore, the novel CMCht/PAMAM dendrimer nanoparticles may be used as targeted drug-delivery carriers to cover a wide range of applications that involve the efficient intracellular delivery of biological agents to modulate the behavior of cells. These might include the use of differentiation factors to act from the inside of the cell or on genetic material. The incorporation of fluorescent labels for live-cell imaging and monitoring of the final intracellular fate of such structures is also possible.

4. Experimental

Synthesis of the CMCht/PAMAM nanoparticles: CMCht with a degree of deacetylation of 80% and degree of substitution of 47% was synthesized by a chemical modification route of chitin (Sigma, Germany) as described by Chen et al. [53]. Starburst PAMAM-carboxylic acid terminated dendrimers, PAMAM-CT (generation 1.5, 20% (w/v) methanolic solution) with an ethylenediamine core were purchased from Aldrich. CMCht/PAMAM dendrimer nanoparticles were prepared in a stepwise manner as follows: i) increasing the generation of the PAMAM-CT (G 1.5), ii) obtaining a PAMAM-methyl ester terminated dendrimer, iii) reaction of PAMAM and CMCht (the reaction occurs by a condensation reaction between the methyl ester and amine groups [54]), and iv) converting the methyl ester groups that do not react into carboxylic groups in the CMCht/PAMAM dendrimer, followed by precipitation. First, the increase of the dendrimers' generation was carried out as follows: an appropriate volume of PAMAM-CT (G 1.5) in methanol was transferred to a 2 mL volumetric flask and the solvent evaporated off under nitrogen gas, and the traces dried under vacuum in order to completely remove the methanol. The starting compound was re-dissolved in ultra-pure water to give a final concentration of 10 mg mL^{-1} and the pH was adjusted to 6.5 with dilute hydrochloric acid solution (Riedel de-Haen, Germany). 1-Ethyl-(3-dimethylaminopropyl) carbodiimide hydrochloride (EDC, Fluka, Slovakia) was then added to the solution at a molar ratio sufficient to modify the carboxylate residue of the dendrimers, and the solution was kept under agitation for 30 min at room temperature. Ethylenediamine (EDA, Sigma, Germany) was added to the solution at a molar ratio equal to that of EDC and left to react for at least 4 h. After this period the excess EDC was removed by dialysis (cellulose tubing, benzoylated for separating compounds with a molecular weight of $\leq$1200 from compounds with a molecular weight >2000, Sigma, Germany). The compound was used without purification in the next step. After preparing the PAMAM-amine terminated compound (PAMAM-AT) an exhaustive alkylation of the primary amines (Michael addition) was performed [55]. An appropriate volume of PAMAM-AT ($\sim$8.4 mmol) was transferred to a 50 mL flask and 30 mL of methanol (Sigma, Germany) and 1.14 mL of methyl methacrylate ($\sim$12.6 mmol, Fluka, Germany) were added. The solution was kept under agitation in a water bath for 24 h at 50 °C, to obtain the PAMAM-methyl ester. The CMCht (100 mg) dissolved in ultrapure water (10 mL) was mixed with the PAMAM-methyl ester dendrimer (50 mg), which was previously dissolved in a 20/80 water/methanol (v/v) solution. The final solution was diluted by adding 30 mL of methanol and kept under agitation for 72 h. After this period, a CMCht/PAMAM dendrimers with carboxylic-terminated groups were obtained as described elsewhere [54]. CMCht/PAMAM dendrimer nanoparticles were then precipitated after addition of an appropriate volume of a saturated Na_2CO_3 (Aldrich, Germany) solution and acetone (Pronalab, Portugal). Some CMCht/PAMAM dendrimer nanoparticles were

mixed with a Dex solution with a final concentration of 5×10^{-4} M under agitation (w/w). The mixture was then added to the precipitation media that consisted of a saturated Na_2CO_3 and acetone solution, under vigorous agitation. Precipitates were collected by filtration and dispersed in ultrapure water for dialysis over a period of 48 h. Both CMCht/PAMAM and Dex-loaded CMCht/PAMAM dendrimer nanoparticles were obtained by freezing the solution at −80 °C and freeze-drying (Telstar-Cryodos-80, Spain) up to 4 d to completely remove the solvent. It is worth noting that the CMCht/PAMAM dendrimer nanoparticles were water-soluble at physiological pH.

Labeling of CMCht/PAMAM Dendrimer Nanoparticles with FITC: A 10 mg mL^{-1} FITC (Sigma, Germany) solution was prepared in anhydrous dimethyl sulfoxide (DMSO, Riedel de-Haen) (dark conditions). Conjugates of CMCht/PAMAM-FITC were prepared by covalently bonding the amine group of CMCht and the isothyocianate group of FITC (thiourea bond). First, a 10 mg mL^{-1} CMCht/PAMAM dendrimer nanoparticle solution was prepared in a carbonate-bicarbonate coupled buffer of pH 9.2. A 50 μL aliquot of the FITC/DMSO solution was then added for each milliliter of the CMCht/PAMAM dendrimer nanoparticle buffered solution under agitation, and the mixture was kept in the dark at 4 °C for 8 h. The FITC-labeled CMCht/PAMAM dendrimer nanoparticle solution was dialyzed against ultra-pure water in order to remove unlinked FITC for 24 h and filtered (pore size <220 nm) in sterile and dark conditions. The final product was obtained as an orange powder after freeze-drying. The labeling efficiency was investigated by FTIR spectroscopy (Perkin-Elmer 1600 series equipment, USA) and UV-vis spectrophotometry (NanoDrop ND-1000; NanoDrop Technologies, USA).

Characterization of the CMCht/PAMAM Dendrimer Nanoparticles: FTIR analyses were performed by means of preparing transparent potassium bromide pellets that contained the samples and using a Perkin–Elmer spectroscope (Perkin–Elmer 1600 series equipment, UK).

The morphology of the nanoparticles was investigated using atomic force microscopy (AFM). The lyophilized CMCht/PAMAM dendrimer nanoparticles were dispersed in ultrapure water to obtain a solution with a final concentration of 1 mg mL^{-1}, and then 20 μL was placed over a 9.9 mm mica disc (Agar Scientific, England) and blow dried with nitrogen gas for subsequent characterization. The samples were analyzed using the Tapping Mode with a MultiMode AFM connected to a NanoScope III controller, both from Veeco, USA, with non-contact silicon nanoprobes (~300 kHz) from Nanosensors, Switzerland. All images were plane-fitted using the third degree-flatten procedure included in the NanoScope software version 4.43r8. The particle size distribution was determined with the same software. The morphology and size of the particles was further analyzed by TEM (Philips CM12, FEI Company, The Netherlands, equipped with a MEGA VIEW-II DOCU camera and Image Software Analyzer SIS NT DOCU). The nanoparticles were stained with 2% phosphotungstic acid and placed on copper grids for further observation. The size of the CMCht/PAMAM dendrimer nanoparticles was also measured in a particle size analyzer (Zetasizer Nano ZS, Malvern Instruments, UK).

In-Vitro Cytotoxicity Screening of the CMCht/PAMAM Dendrimer Nanoparticles: A luminescent cell viability assay based on the ATP quantification was performed by exposing RBMSCs to CMCht/PAMAM dendrimer nanoparticles. Prior to the cell culture studies CMCht, PAMAM-CT G 1.5, and CMCht/PAMAM nanoparticles were sterilized under an ethylene oxide gas atmosphere. RBMSCs were isolated from the femora of 7 week-old male Fischer 344/N rats (SLC Inc. Japan), and expanded in T75 cm^2 culture flasks in the presence of MEM (Nacalai Tesque, Japan) with 15% FBS (JRH Biosciences, USA) and 1% antibiotic-antimycotic (Nacalai Tesque, Japan) solution. The animals were sacrificed by administrating an excess of anaesthesia, in accordance to the Ethics Committee at the Tissue Engineering Research Center (Amagasaki, Japan). After reaching confluency, the cells (passage 1, P1) were released from the substratum and centrifuged at 900 rpm for 5 min. The supernatant was aspirated and cells re-suspended with 10 mL of complete culture medium. The cell concentration was determined using an automatic cell counter (Cell Counter Sysmex F-520, Japan). Viability of the RBMSCs was also analyzed with a NucleoCounter (Chemometec, Denmark), using prior seeding as described elsewhere. [56] RBMSCs were seeded (sub-cultured) in each well of a 96-well TCPS plate at a cell density of 5×10^3 cells mL^{-1}. A solution of CMCht/PAMAM dendrimer nanoparticles at a concentration of 10 mg mL^{-1} was prepared in a complete culture medium. Serial dilutions (1, 0.1, 0.01 mg mL^{-1}) were further prepared using the complete culture medium. Possible changes in the osmolality of the culture media were investigated using an automatic cryoscopic osmometer (OSMOMAT O 30-D, Gonotec, Germany). After a period of 24 h, the culture medium was changed by the respective serial dilutions and the cells cultured under standard culture conditions for 1 and 3 d. A latex rubber extract was used as the positive control for cellular death. Finally, the ATP content was measured by means of performing a CellTiter-Glo luminescent cell viability assay, following the protocol provided by the supplier (Promega Corporation, USA). Luminescence was measured using an opaque-walled multi-well plate in a microplate reader (Wallac ARVOsx 1420, Perkin-Elmer Life and Analytical Sciences, USA). Results were analyzed for statistical significance using a Student's *t*-test with the JMP 5.0.1 software (SAS Institute, Cary, N.C.).

Investigation of the Internalization Efficiency using SaOS-2 Cells and RBMSCs under Fluorescence Microscopy and FACS Analysis: Human osteoblast-like cells (SaOs-2 cells, ECACC, UK) were maintained in T75 cm^2 culture flasks, cultured with basic culture medium (MEM supplemented with 10% FBS and 1% A/B) and passaged after reaching confluence. A cell suspension was prepared and seeded on TCPS coverslips (Sarstedt Inc., USA) in 24-well plates (1×10^4 cells per well) and cultured under standard culture conditions for 24 h. The internalization of the CMCht/PAMAM dendrimer nanoparticles by SaOs-2 cells was assessed after 3, 12, and 24 h, and 14 d. After each time point cells on the TCPS coverslips were fixed with 4% formalin (Sigma, Germany) and the nuclei stained with DAPI blue (100 ng mL^{-1}, Molecular Probes) to assess possible cell morphological changes. Fluorescence was protected by using an antifade agent (ProLong Antifade Kit, Invitrogen, USA), following the supplier procedure, and cells were observed under the fluorescence microscope (AxioImager Z1, Zeiss Inc., Germany).

RBMSCs were isolated from rats and expanded until reaching 80% of confluency. The RBMSCs (P1) were trypsinized and transferred to a 6-well plate (1×10^5 cells per well) and to TCPS coverslips in a 24-well TCPS plate (2×10^4 cells per well) for analysis under FACS and fluorescence microscopy, respectively. For fluorescence microscopy, RBMSCs were cultured in a MEM complete culture medium containing 0.1 mg mL^{-1} of FITC-labeled CMCht/PAMAM dendrimer nanoparticles for a period of 12 h until 14 d. For FACS analysis, RBMSCs were cultured in the presence of 0.01 mg mL^{-1} of FITC-labeled CMCht/PAMAM dendrimer nanoparticles. All experiments were carried out in triplicate. The samples for fluorescence microscopy were prepared as follows: each well was washed with 1 mL of PBS, and cells were fixed with 4% formalin (Nacalai Tesque, Japan) for 10 min at 4 °C followed by washing each well twice with PBS. After that cells were incubated with 0.5 mL of PBS that contained Texas Red-X phalloidin (Molecular Probes, Invitrogen, USA) and Hoechst 33258 (Invitrogen, USA) for staining the actin filaments of the cytoskeleton and nuclei of the cells, respectively. The protocols provided by the supplier were followed with few modifications. The permeabilization of cells with Triton X-100 was not carried out to avoid any undesired effect on the integrity of the cells' nuclei. TCPS coverslips were washed once with PBS and fluorescence protected using the ProLong antifade kit. The specimens were observed under a fluorescence microscope (Olympus IX70, Olympus Co. Ltd, Japan). FACS analysis was carried out as follows: each well of the 6-well plate was washed with 2 mL of PBS. PBS was then aspirated and cells were released from the substratum as described above. Afterwards, 3.5 mL of MEM complete medium was added to each well and samples were transferred to a 15 mL Falcon. After centrifugation at 900 rpm for

5 min, cells were re-suspended in 0.5 mL of complete culture medium and passed through cell strainers [57]. Afterwards, 1 μL of PI (Nacalai Tesque, Japan) was added to each sample to determine the number of live cells. After this step, cells were loaded into a FACSCalibur flow cytometer (BD Biosciences Imunocytometry Systems, USA) and analyzed with a minimum of 10 000 events counting. A Calibrite beads three-color kit (BD CaliBRITE beads, USA) was used to adjust the equipment instrument settings before samples were run on the flow cytometer. Finally, the fluorescence-activated cell sorting (FACS) data was treated using the FLOWJO software.

Investigation of the Effect of Colchicine and Apyrase on the Internalization Efficiency of FITC-Labeled CMCht/PAMAM Dendrimer Nanoparticles by RBMSCs: A cell suspension of RBMSCs (P1) in MEM complete culture medium was transferred to a 6-well (1×10^5 cells per well) plates and TCPS coverslips in a 24-well TCPS plate (2×10^4 cells per well) for analysis under FACS and fluorescence microscopy, respectively. Stock solutions of 10 U mL^{-1} apyrase (Nacalai Tesque, Japan) and 10×10^{-6} M colchicine (Nacalai Tesque, Japan) were prepared in a PBS solution. Cells were incubated under standard culture conditions and after 24 h the culture medium was replaced by a different complete culture medium that contained the FITC-labeled CMCht/PAMAM dendrimer nanoparticles (0.01 and 0.1 mg mL^{-1}), and in the presence of 1×10^{-6} M colchicine or 0.1 U mL^{-1} apyrase or both, for a period of 12 h to 14 d. Controls for internalization were performed by culturing RBMSCs in complete culture medium and in the presence of both colchicine and apyrase. All experiments were carried out in triplicate. After each time period, specimens were prepared as described previously. The tendency of FITC-labeled CMCht/PAMAM dendrimer nanoparticles to be internalized by RBMSCs was investigated by means of FACS analysis.

Investigation of the Dex Release from CMCht/PAMAM Dendrimer Nanoparticles: The amount of Dex released from the nanoparticles was measured using an HPLC (ASI-Knauer, Germany) with an UV detector set at 246 nm. The mobile phase consisted of acetonitrile/acetate buffer (2×10^{-3} M, pH 4.8 adjusted with glacial acetic acid) (50 : 50, v/v) at flow rate of 1 mL min^{-1}. In brief, Dex release was studied after dissolution of 10 mg of Dex-loaded CMCht/PAMAM dendrimer nanoparticles in 10 mL of a PBS (pH 7.4, Sigma, USA) solution in the absence or presence of 15% FBS. Sodium azide 0.01% (w/v, Merck, Germany) was added to the buffer. The in-vitro release studies were performed at 37 °C and 60 rpm for times that ranged from 1 h to 7 d. At set time intervals, 1 mL of sample was taken for analysis and the same volume replaced by the respective buffer solution. Prior analysis, samples were centrifuged at 2000 rpm for 10 min. A solution with sample/acetonitrile/acetate buffer (50:25:25 v/v) was prepared for further analysis. A Eurospher 100 C-18 analytical column (ASI-Knauer, Germany) was used. The retention time of Dex was 4 min. A calibration curve was obtained following the method described by Sun et al. [58]. Results were expressed as an average ± standard deviation, $n = 6$.

Evaluation of Osteogenic Differentiation of the RBMSCs Cultured in the Presence of CMCht/PAMAM Dendrimer Nanoparticles Loaded with Dex, In Vitro: RBMSCs were isolated from F344/N rats and expanded as described above. RBMSCs (P1) were cultured in a TCPS 24-well plate at a cell density of 2×10^4 cells per well, and cultured in a complete MEM for 24 h. After that time, the culture medium was replaced by a different culture media, and RBMSCs were cultured for times up to 14 d. The effect of the concentration of CMCht/PAMAM dendrimer nanoparticles loaded with Dex on the RBMSCs osteogenic differentiation was investigated. Dex-loaded CMCht/PAMAM dendrimer nanoparticles were dissolved in MEM supplemented with 0.28×10^{-3} M ascorbic acid (Wako Pure Chemicals, Japan) and 10×10^{-3} M β-glycerophosphate (Sigma, USA) at a final concentration of 0.01 and 1 mg mL^{-1}. RBMSCS were also cultured in a complete MEM, complete MEM that contained 1 mg mL^{-1} of CMCht/PAMAM dendrimer nanoparticles, and complete MEM that contained 10×10^{-3} M β-glycerophosphate (negative controls). Complete MEM supplemented with 10^{-8} M Dex, 0.28×10^{-3} M ascorbic acid and 10×10^{-3} M β-glycerophosphate was used as the positive control for osteogenic differentiation. Culture media were changed every 2–3 d. All experiments were carried out three times using a minimum of four replicates per experimental condition.

Alizarin red S staining was performed to investigate possible calcium deposition after 14 d of culturing. RBMSCs were washed twice with PBS and fixed with 95% ethanol for 15 min. The fixed cells were then washed once with PBS and stained with 5 mg mL^{-1} of Alizarin red S in PBS for 5 min at room temperature. A washing step followed with ultra-pure water and the sample was mounted with Crystal/Mount (BiomedaCorporation, USA) for observation under the phase contrast microscope (Olympus CK40, Olympus Co. Ltd, Japan).

For the ALP staining, the cells were washed twice with PBS after each culture period. Cells were fixed with 4% paraformaldehyde (Nacalai Tesque, Japan) for 15 min at 4 °C and then washed twice with AMP buffer (56×10^{-3} M of 2-amino-2 methylpropane-1,3-diol in ultrapure water, pH 9.9). The cells were then soaked in a staining solution of 0.5 mg naphthol AS-MX phosphate and 0.5 mg of fast red violet LB salt per millilitre in AMP buffer. Cells were incubated for 10 min at room temperature, washed with PBS, and mounted (BiomedaCorporation, USA) for observation under the phase contrast microscope.

DNA quantification was performed using Hoechst 33258 (Nacalai Tesque, Japan), as previously described elsewhere [59].

ALP was measured to evaluate osteoblast differentiation. The samples used for DNA quantification assay were used to determine the ALP levels. Prior to analysis, the samples were centrifuged at 10 000 rpm for 1 min at 4 °C. To each well of a 96-well plate was added an aliquot of supernatant and *p*-nitrophenyl phosphate substrate (ZYMED Laboratories, Invitrogen, USA). The plate was then incubated in the dark for 30 min at 37 °C. After the incubation period, the reaction was stopped with 1 M NaOH (Panreac). Standards were prepared with *p*-nitrophenol (pNP). Triplicates were made for each sample and standard. Absorbance was read at 405 nm (Wallac ARVOsx 1420, Perkin–Elmer Life and Analytical Sciences, USA), and sample concentrations were read off from the standard graph. Enzyme activity was expressed either as nmol of pNP released per well per 30 min and normalized by DNA content.

The samples used for ALP activity were treated with a 20% formic acid solution immediately after concluding the assay and stored at 4 °C for 2–3 d. Samples were then centrifuged at 3000 rpm for 10 min at 4 °C and the supernatant passed through a Sephadex G-25 column (GE healthcare, Sweden) for desalting. The filtered samples were concentrated in a SPD SpeedVac attached to a UV Vacuum System (Thermo Electron Corporation, USA), prior to osteocalcin quantification. Finally, the osteocalcin content was determined by performing an ELISA, and using a Rat Osteocalcin EIA kit (N° BT-460, Biomedical Technologies Inc., USA). The experimental procedure was carried out following the instructions provided by the supplier. A 100 ng mL^{-1} standard solution of human osteocalcin was used to construct the standard curve. Data was read off from the standard graph and expressed as nanograms of deposited osteocalcin per microgram of DNA.

Received: January 31, 2008
Published online: June 10, 2008

[1] D. A. Tomalia, J. M. Frechet, *Prog. Polym. Sci.* **2005**, *30*, 217.
[2] S. Svenson, D. A. Tomalia, *Adv. Drug Delivery Rev.* **2005**, *57*, 2106.
[3] D. A. Tomalia, *Prog. Polym. Sci.* **2005**, *30*, 294.
[4] R. Esfand, D. A. Tomalia, *Drug Discovery Today* **2001**, *6*, 427.
[5] R. Jevprasesphant, J. Penny, D. Attwood, N. B. Mckeown, A. D'Emanuele, *Pharm. Res.* **2003**, *20*, 1543.
[6] A. D'Emanuele, R. Jevprasesphant, J. Penny, D. Attwood, *J. Controlled Release* **2004**, *95*, 5447.

ADVANCED FUNCTIONAL MATERIALS

[7] H. Sashiwa, Y. Shigemasa, R. Roy, *Carbohydr. Polym.* **2002**, *49*, 195.
[8] D. M. Domanski, B. Klajnert, M. Bryszewska, *Bioelectrochemistry* **2004**, *63*, 193.
[9] D. V. Sakharov, A. F. H. Jie, D. V. Filippov, M. E. A. Bekkers, J. H. van Boom, D. C. Rijken, *FEBS Letters* **2003**, *573*, 6.
[10] D. Luo, K. Haverstick, N. Belcheva, E. Han, W. M. Saltzman, *Macromolecules* **2002**, *35*, 3456.
[11] N. Hata, M.-H. Kim, K. Isoda, M. Kino-Oka, M. Kawase, K. Yagi, M. Taya, *J. Biosci. Bioeng.* **2004**, *97*, 233.
[12] C. C. Lee, J. A. MacKay, J. M. Fréchet, F. C. Szoka, *Nat. Biotechnol.* **2005**, *23*, 1517.
[13] S. H. M. Sontjens, D. L. Nettles, M. A. Carnahan, L. A. Setton, M. W. Grinstaff, *Biomacromolecules* **2006**, *7*, 310.
[14] D. A. Tomalia, *Mater. Today* **2005**, *8*, 34.
[15] N. Malik, R. Wiwattanapatapee, R. Klopsch, K. Lorenz, H. Frey, J. W. Weener, E. W. Meijer, W. Paulus, R. Duncan, *J. Controlled Release* **2000**, *65*, 133.
[16] A. P. Marques, R. L. Reis, *Mater. Sci. Eng. C* **2005**, *25*, 215.
[17] H. P. Wiesmann, N. Nazer, C. Klatt, T. Szuwart, U. Meyer, *J. Oral Maxillofacial Surg.* **2003**, *61*, 1455.
[18] M. X. Tang, C. T. Redemann, F. C. Szoka, *Bioconjug. Chem.* **1996**, *4*, 372.
[19] J. Li, Y. Du, H. Liang, *Polym. Degrad. Stab.* **2007**, *92*, 515.
[20] H. Gao, W. Shi, L. B. Freund, *Proc. Natl. Acad. Sci. USA* **2005**, *102*, 9469.
[21] H. Sato, Y. Sugiyama, A. Tsuji, I. Horikoshi, *Adv. Drug Delivery Rev.* **1996**, *19*, 445.
[22] A. P. Zhu, M. B. Chan-Park, S. Dai, L. Li, *Colloids Surf. B* **2005**, *43*, 143.
[23] A. P. Zhu, L. Jianhong, Y. Wenhui, *Carbohydr. Polym.* **2006**, *63*, 89.
[24] H. M. Brothers II, L. T. Piehler, D. A. Tomalia, *J. Chromatogr. A* **1998**, *814*, 233.
[25] J. S. Ryu, G. M. Lee, *Biotechnol. Bioeng.* **1997**, *55*, 565.
[26] M. Huang, E. Khor, L.-Y. Lim, *Pharm. Res.* **2004**, *21*, 344.
[27] A. P. Marques, R. L. Reis, J. A. Hunt, *Biomaterials* **2002**, *23*, 1471.
[28] D. Fischer, Y. Li, B. Ahlemeyer, J. Krieglstein, T. Kissel, *Biomaterials* **2003**, *24*, 1121.
[29] S. Choksakulnimitr, S. Masuda, H. Tokuda, Y. Takakura, M. Hashida, *J. Controlled Release* **1995**, *34*, 233.
[30] D. M. Domanski, B. Klajnert, M. Bryszewska, *Bioelectrochemistry* **2004**, *63*, 189.
[31] D. Luo, W. M. Saltzman, *Nat. Biotechnol.* **2000**, *18*, 893.
[32] R. Jevprasesphant, J. Penny, D. Attwood, A. D'Emanuele, *J. Controlled Release* **2004**, *97*, 259.
[33] L. Prinzen, R.-J. J. H. M. Miserus, A. Dirksen, T. M. Hackeng, N. Deckers, N. J. Bitsch, R. T. A. Megens, K. Douma, J. W. Heemskerk, M. E. Kooi, P. M. Frederik, D. W. Slaaf, M. A. M. J. van Zandvoort, C. P. M. Reutelingsperger, *Nano Lett.* **2007**, *7*, 93.
[34] X. Huo, X.-J. Xu, Y.-W. Chen, H.-W. Yang, Z.-X. Piao, *World J. Gastroenterol.* **2004**, *10*, 1666.
[35] K. J. Thompson, M. G. Fried, Z. Ye, B. Phillip, J. R. Connor, *J. Cell Sci.* **2002**, *115*, 2165.
[36] F. Yokoya, N. Imamoto, T. Tachibana, Y. Yoneda, *Mol. Biol. Cell* **1999**, *10*, 1119.
[37] A. Yan, B. W. Lau, B. S. Weissman, I. Kulaots, N. Y. C. Yang, A. B. Kane, R. H. Hurt, *Adv. Mater.* **2006**, *18*, 2373.
[38] E. Kallard, K. J. Johnson, K. Boekelheide, *Biol. Reprod.* **1993**, *48*, 143.
[39] M. A. Tsai, R. E. Waugh, P. C. Keng, *Biophys. J.* **1998**, *74*, 3282.
[40] J. T. Trevors, *J. Biochem. Biophys. Methods* **2003**, *57*, 87.
[41] J. Beresford, C. Joyner, C. Devlin, J. Triffitt, *Archs Oral Biol.* **1994**, *39*, 941.
[42] J. Blum, M. Parrott, A. Mikos, M. Barry, *J. Orthopaedic Res.* **2004**, *22*, 411.
[43] M. Eijken, M. Koedam, M. van Driel, C. Buurman, H. Pols, J. van Leeuwen, *Mol. Cell. Endocrinol.* **2006**, *248*, 87.
[44] R. Hayashi, H. Wada, K. Ito, I. Adcock, *Eur. J. Pharmacol.* **2004**, *500*, 51.
[45] C. Vorgias, G. Perides, P. Traub, C. Sekeris, *Biosci. Rep.* **1988**, *8*, 193.
[46] P. Kallinteri, S. G. Antimisiaris, D. Karnabatidis, C. Kalogeropoulou, I. Tsota, D. Siablis, *Biomaterials* **2002**, *23*, 4819.
[47] G. Beck, B. Zerler, E. Moran, *Proc. Natl. Acad. Sci. USA* **2000**, *97*, 8352.
[48] E. Uchimura, H. Machida, N. Kotobuki, T. Kitamura, M. Ikeuchi, M. Hirose, J. Miyake, H. Ohgushi, *Calcif. Tissue Int.* **2003**, *73*, 575.
[49] N. Jorgensen, Z. Henriksen, O. Sorensen, R. Civitelli, *Steroids* **2004**, *69*, 219.
[50] N. Jaiswal, S. E. Haynesworth, A. I. Caplan, S. P. Bruder, *J. Cell Biochem.* **1997**, *64*, 295.
[51] H. Harris, *Clin. Chim. Acta.* **1989**, *186*, 133.
[52] N. Ogston, A. Harrison, H. Cheung, B. Ashton, G. Hampson, *Steroids* **2002**, *67*, 895.
[53] X.-G. Chen, H.-J. Park, *Carbohydr. Polym.* **2003**, *53*, 355.
[54] H. Sashiwa, Y. Shigemasa, R. Roy, *Carbohydr. Polym.* **2002**, *47*, 201.
[55] D. A. Tomalia, A. M. Naylor, W. A. Godard, *Angew. Chem. Int. Ed. Engl.* **1990**, *29*, 138.
[56] N. Kotobuki, M. Hirose, H. Machida, Y. Katou, K. Muraki, Y. Takakura, H. Ohgushi, *Tissue Eng.* **2005**, *11*, 663.
[57] N. Kotobuki, M. Hirose, Y. Takakura, H. Ohgushi, *Artificial Organs* **2004**, *28*, 33.
[58] J.-J. Sun, Y. Liu, W.-J. Kong, P. Jiang, W. Jiang, *Clin. Med. J.* **2007**, *120*, 2284.
[59] S. Kitamura, H. Ohgushi, M. Hirose, H. Funaoka, Y. Takakura, H. Ito, *Artificial Organs* **2004**, *28*, 72.